Clumped isotopes in globally distributed Holocene coccoliths reveal their habitat depth

Luz María Mejía[1,2*], Stefano M. Bernasconi[1], Hongrui Zhang[1], José Guitián[1,3], Alvaro Fernandez[1,4], Ivan Hernández-Almeida[1], Madalina Jaggi[1], Negar Haghipour[1], Heather Stoll[1]

[1] Geological Institute, ETH Zürich, Sonneggstrasse 5, ETH, 8092, Zürich, Switzerland.
[2] Now at MARUM, University of Bremen, 28359 Bremen, Germany
*corresponding author: lmejia@marum.de
[3] Now at Centro de Investigación Mariña, Universidade de Vigo, GEOMA, Vigo, 36310, Spain
[4] Now at Instituto Andaluz de Ciencias de la Tierra, Av. de las Palmeras, 4, 18100 Armilla, Granada, Spain

This is a non-peer reviewed preprint submitted to EarthArXiv. It was submitted to EPSL (Earth and Planetary Science Letters) and is currently under review.

Clumped isotopes in globally distributed Holocene coccoliths reveal their habitat depth

Luz María Mejía[1,2], Stefano M. Bernasconi[1], Hongrui Zhang[1], José Guitián[1,3], Alvaro Fernandez[1,4], Ivan Hernández-Almeida[1], Madalina Jaggi[1], Negar Haghipour[1], Heather Stoll[1]

Reliable temperature reconstructions are necessary to improve climate reconstructions and comparisons with paleoclimate model simulations. Most existing paleotemperature proxies are based on organic and inorganic remains of marine organisms. Despite the evidence that the habitat depth of coccolithophores and other phytoplankton depend on their ability to balance light, nutrients, and grazing pressure, calibrations of proxies based on photosynthesizers often assume they live in the surface ocean. Here we present the first globally distributed dataset of core top multi-species coccolith clumped isotopes (Δ_{47}), which show a clear latitudinal thermal gradient and demonstrate coccolith Δ_{47} sensitivity to temperature. The application of the most recent Δ_{47}-temperature calibration for marine biogenic carbonates yield calcification temperatures implying deep habitats for tropical coccolithophores (from ~50 to up to ~150 m), which could photosynthesize with 1-10% of surface photosynthetic active radiation (PAR) levels. Given the low upper ocean temperature gradient of well-mixed high-latitude locations and the current uncertainties of Δ_{47} thermometry, coccolith Δ_{47} cannot be used to reliably constrain a specific habitat depth in these locations. Nevertheless, they are a good indicator of paleotemperatures of the mixed layer. We also use coccolith Δ_{47} to derive the first regression relating core top coccolith Δ_{47} and sea surface temperatures (SST). Although this formulation cannot be considered a proper coccolith-specific Δ_{47} calibration, since it ignores coccolithophore's potential for calcification at depth, it facilitates comparison

with temperature proxies like $U_{37}^{k'}$, which are regressed to SST, rather than production temperature.

Keywords: Clumped isotopes, Coccolithophores, Core top, Habitat depth, Temperature reconstructions

[1] Geological Institute, ETH Zürich, Sonneggstrasse 5, ETH, 8092, Zürich, Switzerland.
[2] Now at MARUM, University of Bremen, 28359 Bremen, Germany
[3] Now at Centro de Investigación Mariña, Universidade de Vigo, GEOMA, Vigo, 36310, Spain
[4] Now at Instituto Andaluz de Ciencias de la Tierra, Av. de las Palmeras, 4, 18100 Armilla, Granada, Spain

1. Introduction

Estimates of past sea surface temperatures (SST) are an important paleoclimate proxy goal. The most widely used geochemical SST proxies are either based on organic biomarkers produced by coccolithophores (alkenone unsaturation index - $U_{37}^{k'}$) and archaea (archaeal tetraether index -TEX_{86}-), or on biominerals produced by planktonic foraminifera ($\delta^{18}O$, Mg/Ca and more recently, clumped isotopes -Δ_{47}-). Since alkenones are produced by coccolithophores, which rely on light availability to photosynthesize and lack any motile apparatus during their diploid phase, $U_{37}^{k'}$ is often assumed to be the most reliable indicator of temperatures at the ocean's surface. Conversely, TEX_{86} may also record subsurface ocean temperatures, as the archaea that produce these biomarkers can live throughout the water column (Ho and Laepple, 2016; Rommerskirchen et al., 2011; Schouten et al., 2013; Tierney et al., 2017), and even planktic foraminifera inferred to dwell in the surface mixed layer may span depths from 15 to up to ~200 meters in different oceanographic settings and seasons (Kretschmer et al., 2018; Rebotim et al., 2017).

Reconstructions of ocean temperatures from these proxies are used in climate models to access their performance and to understand past climate evolution and Earth climate sensitivity (e.g. Lunt et al., 2021; Zhu et al., 2019). However, if instead of SST, some of these proxies were actually indicators of deeper water conditions, climate modelers

should consider depth differences in their calibration efforts. Plankton sampling shows that placolith-bearing coccolithophores, including those of alkenone producers, are present at depths ranging from the surface to 200-300 m in different ocean settings (Balch et al., 2019; Beaufort et al., 2008; Liu et al., 2021; Poulton et al., 2017). While the presence of cells at depth is not necessarily indicative of significant cell growth, the shallowest layer is also not always favorable for growth because it can be nutrient-depleted and high light intensities and UV radiation can damage photosystem II and inhibit its repair cycle (Bouchard' et al., 2006; Guan and Gao, 2010). In addition to alkenones, coccolithophores produce calcite platelets termed coccoliths, which are well preserved in the geological record, and can be used to infer their habitat's conditions in the past.

Clumped isotope (Δ_{47}) thermometry is a technique that estimates temperatures of calcification by comparing the excess abundance of ^{13}C-^{18}O bonds in the carbonate with that expected from a stochastic distribution (Eiler, 2011, 2007; Schauble et al., 2006). In contrast to foraminiferal $\delta^{18}O$ and Mg/Ca, it is independent of seawater chemistry (Ghosh et al., 2006), and Δ_{47} thermometry in planktic and benthic foraminifera is therefore emerging as an important paleoceanographic proxy (e.g. Evans et al., 2018; Leutert et al., 2020; Meckler et al., 2022; Meinicke et al., 2021, 2020; Peral et al., 2022, 2018; Piasecki et al., 2019; Rodríguez-Sanz et al., 2017). Despite the abundance of coccoliths in Cenozoic sediments and the constraint that they must be produced in the photic zone, the potential of their Δ_{47} thermometry has not yet been rigorously evaluated in ocean sediment samples. A culture study showed that coccolith Δ_{47} correlates closely with temperature and found no significant differences in the relationship among different species (Katz et al., 2017).

In order to verify the relationship between temperature and sedimentary coccolith Δ_{47}, we measured Δ_{47} on globally distributed Holocene multispecies coccolith fractions, which represent natural populations, and would be the most readily obtained fraction for future paleoceanographic studies. We also use our coccolith Δ_{47} to evaluate coccolithophores' habitat depth in different oceanographic settings. For this, we apply the most recent biogenic Δ_{47} calibration (Meinicke et al., 2021) to derive coccolith calcification temperatures. We then compare these temperatures with the vertical distribution of ocean temperatures in the modern upper water column during the season of production, and with alkenone $U_{37}^{k'}$-derived temperatures from the same samples calculated using core top calibrations regressed to SSTs (Müller et al., 1998; Tierney and Tingley, 2018). This assessment of likely calcification and habitat depth may improve interpretation of temperatures attained from both alkenones and coccolith Δ_{47}, facilitating more robust proxy intercomparison and more meaningful information for data-model comparisons.

2. Materials and Methods

2.1. Sediment samples

We chose a set of 12 sites distributed around the world, including locations with various oceanographic conditions (Fig. 1; Supplementary Table A). These comprised: a) three tropical Equatorial Pacific sites influenced by upwelling (IODP U1337, IODP 1338, and ODP 1226); b) two tropical oligotrophic sites, including one in the Caribbean Colombian basin (ODP Site 999), and one in the southern South China Sea (ODP 1143); c) three in the North Atlantic at mid-latitude (northeast of the Azores: IODP U1312) and at high latitudes (Rockall Plateau: ODP 982, and Iceland Plateau: ODP 985); d) one in

the South Atlantic in the northwestern flank of the Walvis Ridge (ODP 1266); and e) three in the Southern Ocean (western Pacific sector in the Subantarctic zone: ODP Site 1122, Atlantic sector in the Polar Frontal zone: ODP 1092, and Atlantic sector in the Antarctic zone: ODP 1093). We targeted mid to late Holocene sediments with a modest to high carbonate content so that microfiltration would yield sufficient coccolith fraction for clumped isotope analyses. The age of each sample was determined by radiocarbon analysis of mixed species of planktonic foraminifera (Supplemetary Table B) in the ETH laboratory of Ion Beam Physics (LIP) following established methodologies (McIntyre et al., 2017).

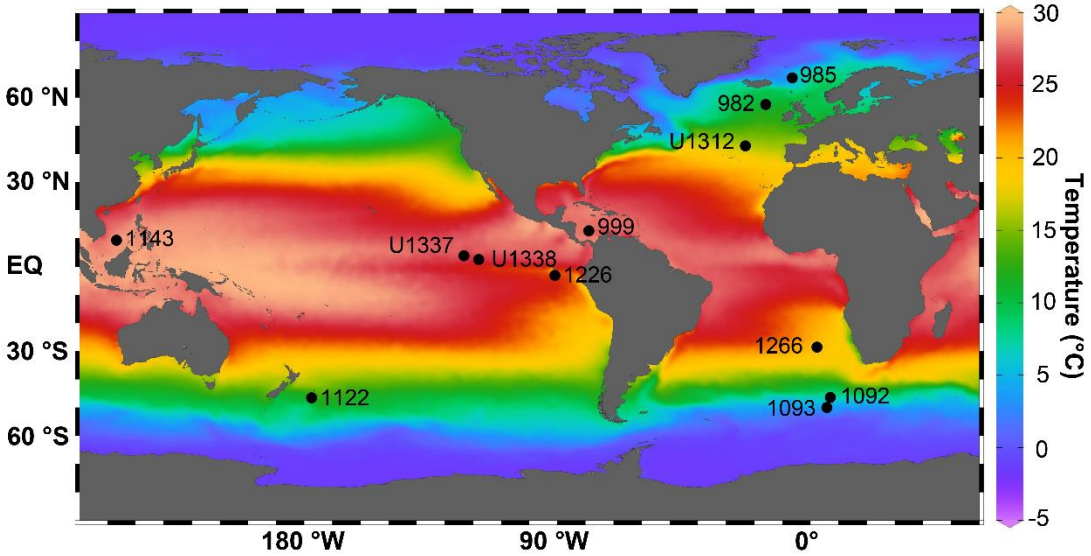

Fig. 1. Location of mid to late Holocene sediment Sites in this study on a global mean surface temperature map (World Ocean Atlas -WOA, 2018) generated using ODV (Schlitzer, 2021).

2.2. Alkenone thermometry

Freeze-dried bulk samples were extracted via accelerated solvent extraction, using a 5:1 mixture of dichloromethane (CH_2Cl_2) and methanol (MeOH) at 100°C in three 10-minute static cycles, using a ThermoFisher 350 Accelerated Solvent Extractor (ASE). The

total lipid extract was separated into hydrocarbon, ketone and polar fractions using silica gel column chromatography. The ketone fraction was analyzed following the methods detailed in Guitián and Stoll (2021) using a Thermo Scientific Trace 1310 Gas Chromatograph (GC) coupled to a flame ionization detector. The precision, estimated from measurements of an in-house alkenone internal standard, was 0.012 $U_{37}^{k\prime}$ units (0.36°C calculated with the calibration of Müller et al., 1998). Abundances of $C_{37:2}$ and $C_{37:3}$ were used to calculate the alkenone unsaturation index ($U_{37}^{k'}$). We applied the most widely used calibrations to estimate SSTs from $U_{37}^{k'}$, including the core top (Müller et al., 1998), the Bayspline (Tierney and Tingley, 2018), and the 55a *Emiliania huxleyi* batch culture (Prahl et al., 1988) calibrations. ODP Sites 999 and 1092 had insufficient alkenones for temperature determination.

2.3. Coccolith clumped isotope thermometry

2.3.1. Organic matter removal

The determination of clumped isotopic composition of carbonates by mass spectrometry can be influenced by contaminants which produce isobaric interferences on the m/z 47 ion beam. To eliminate potential contaminants, we used the bulk sediment extracted for alkenone analysis, i.e. free of extractable lipids. From this material, we obtained a coccolith-enriched <11 µm size fraction by microfiltration in an ammonia solution (0.5%) pre-saturated with respect to carbonate. The remaining organic matter in this fraction was oxidized for four hours using 500 mL of an ammonia-buffered (pH 8-9) 10% hydrogen peroxide (H_2O_2) solution. For organic carbon-rich samples (i.e. U1337 and U1338), a double oxidation step was necessary. To test if the extraction procedure alters the isotopic composition of the samples, we applied the ASE extraction to the

189 international standard ETH 3 because it is a chalk mainly composed of coccoliths, and is
190 very similar to our samples (Bernasconi et al., 2021). The H_2O_2 oxidation was tested in a
191 randomly-chosen sample from which we had abundant material (ODP Site 1266). No
192 effect was observed on measured $\delta^{18}O$, $\delta^{13}C$ and Δ_{47} after solvent extraction nor H_2O_2
193 oxidation (Supplementary Table C).
194

195 *2.3.2. Coccolith size fraction separation*

196 Since all samples were younger than 8700 years (Supplementary Table B), we expect
197 negligible input of authigenic carbonate in the small fraction (<2 µm). Therefore, for most
198 samples we did not eliminate the <2 µm fraction. Rather, we aimed to limit the
199 contribution from large fragments of non-coccolith carbonate, such as foraminifera. We
200 used light microscopy to determine the largest coccolith size, which would exclude
201 foraminifera fragments. When necessary, the <11 µm fraction was filtered again at 8 or
202 10 µm. The filtered samples were then washed three times in Milli-Q water to eliminate
203 the ammonia, dried at 50° C, and homogenized prior to Δ_{47} analysis.

204 We attempted to eliminate the <3 µm size fraction in the two tropical oligotrophic
205 samples (ODP Site 999 and 1143), as light microscopy showed they were enriched in the
206 deep photic species *Florisphaera profunda*. We used a mix of centrifugation (seven
207 repetitions at 2800 RPM for 2 minutes, to eliminate fragments <2 µm) (Zhang et al., 2021)
208 followed by microfiltration at 3 µm. Due to the small sample size, we could not obtain
209 enough purified 3-8 µm coccoliths for ODP Site 999, and therefore we report the Δ_{47}
210 results of the <11 µm fraction.

211 The presence of non-coccolith carbonate, like foraminifera fragments, could bias Δ_{47}-
212 temperature estimations, since they may not share the same habitat temperature. We used
213 scanning electron microscopy (SEM) and trace element analysis (Sr/Ca, Mg/Ca, Al/Ca

and Mg/Al) to determine if non-identifyable fragments, mostly of sizes <2 µm, were originated from broken coccolithophores or foraminifera. Results are shown in Supplementary Note A, Table D, and Fig. A. For this, we dissolved 300-380 µg of final coccolith separations using 2% HNO_3 for ~15 min, and determined element ratios using an Agilent 8800 Triple Quadrupole ICP-MS, using intensity ratio calibration as described in Mejía et al. (2014).

2.3.3. Clumped isotope measurements

Clumped isotopes, $\delta^{18}O$ and $\delta^{13}C$ from coccolith separations were measured using a Kiel IV-Thermo Fisher Scientific MAT 253 system with the LIDI protocol (Müller et al., 2019). The Kiel IV device includes a custom built PoraPakQ trap held a –40 °C to eliminate potential organic contaminants. Prior to each sample run, the pressure-dependent backgrounds are determined on all beams to correct for non-linearity effects in the mass spectrometer. During each run of 46 positions, 3 replicates of 8 different samples, 5 replicates of the carbonate standards ETH-1 and ETH-2, and 10 replicates of ETH-3, are analyzed for data normalization. Two replicates of the international standard, IAEA C2, are analyzed with each run to monitor the long-term reproducibility of the method. For each sample of this study 11-21 replicate measurements (average of 15) were conducted, with sample amounts adjusted to yield 90-110 µg of $CaCO_3$ per replicate. Samples were measured over 19 months and the data were processed with the software Easotope (John and Bowen, 2016). Replicates with 49-parameter values (John and Bowen, 2016) >2 or Δ_{48} offset > 2 ‰ were discarded due to potential sample contamination.

We report Δ_{47} in the I-CDES scale which is defined with the three carbonate standards ETH-1 (Δ_{47}=0.2052‰), ETH-2 (Δ_{47}=0.2085‰), and ETH-3 (Δ_{47}=0.6132‰) (Bernasconi

et al., 2021). Long-term external standard deviation of the international standard IAEA C2 was: $\delta^{13}C$=0.03 ‰, $\delta^{18}O$=0.04‰, Δ_{47}=0.024 ‰; n = 322. Analytical errors of Δ_{47} estimates are reported at the 95% confidence interval (CI) (Fernandez et al., 2017).

2.3.4. Estimation of coccolith calcification temperatures from Δ_{47}

The most reliable estimates of coccolith calcification temperatures would be achieved by applying a statistically well-constrained Δ_{47}-calibration based on coccolithophores grown at known temperatures, and normalized to the I-CDES using carbonate standardization. Unfortunately, the only published coccolith-specific calibration (Katz et al., 2017) was carried out before the introduction of the I-CDES standardization. Thus, calcification temperatures estimated with this calibration have a poorly constrained source of uncertainty (Bernasconi et al., 2021). In addition, it only includes a small number of samples (n=11) with limited replication and a limited range of growth temperatures, which increases the uncertainty of the slope and of the confidence interval. Therefore, we estimated coccolith calcification temperatures using this calibration, but due to the uncertainties, we discuss them only in the Supplementary Information.

The latest published abiogenic carbonate Δ_{47} calibration (Anderson et al., 2021) has the advantage of using the same carbonate standardization (ETH-1, 2 and 3) and processing techniques as those used in this study. To reduce a possible bias induced by the few high temperature datapoints (1-2 °C) we recalculated the published equation using the regression of York et al. (2004) applied to the subset of 23 laboratory-grown and natural samples, which included only temperatures relevant for coccolithophore environments (0.5-36.1 °C). The larger number of datapoints of this calibration translates into smaller uncertainties in temperature estimates. Moreover, temperatures used for this calibration are experimentally determined or directly measured. The main disadvantage

is that this calibration is only based on abiogenic calcite, and biomineralization is a process which could deviate from the expected equilibrium Δ_{47}-temperature relationships (e.g. some corals; Fiebig et al., 2021; Spooner et al., 2016).

The latest foraminiferal core-top based clumped isotope calibration (Meinicke et al., 2021) includes globally distributed planktonic and benthonic species (Meinicke et al., 2020; Peral et al., 2018; Piasecki et al., 2019) , and is directly comparable to our data, as standardization, correction and processing followed the same methodology. Although not derived from coccolithophore calcite, this calibration does consider potential effects of biomineralization. The main uncertainty of this calibration is that the used temperature is not experimentally-derived or directly measured, but rather calculated from foraminifera oxygen isotope composition. However, it includes by far the largest sample set (n=78) and replicate numbers, rendering the calibration the most statistically robust. Furthermore, it has been applied to extinct biomineralizers or other organisms which are not part of the calibration set, under the assumption that the regression is relevant broadly for marine biomineralization (Agterhuis et al., 2022; Caldarescu et al., 2021; Leutert et al., 2021; Meckler et al., 2022). Based on the above considerations, we will focus on calcification temperatures estimated using the Meinicke et al. (2021) calibration, which, until a coccolith-specific calibration is available, can be considered the most reliable (see also Meckler et al., 2022).

2.4. Reconstruction of coccolithophores' habitat depth

Possible coccolith calcification temperatures for each location are defined by the temperature range in the euphotic zone during the season of maximum production. Therefore, assuming no significant vital effects on coccolith Δ_{47}, as suggested by all

previous studies (Drury and John, 2016; Katz et al., 2017; Tagliavento et al., 2019; Tripati et al., 2010), we use the calcification temperatures determined with the Meinicke et al. (2021) calibration to estimate the average habitat depth of coccolithophores at each location. This is done by comparing the Δ_{47}-calcification temperature with the vertical temperature distribution in the water column during the season of main coccolithophore production for each Site, which is taken from the World Ocean Atlas -WOA- (2018). The shallowest and deepest limits are determined from the warmest and coldest Δ_{47}-temperatures determined from the temperature uncertainty at the 95% CI.

Previous studies of Δ_{47} in monospecific planktic foraminifera have relied on $\delta^{18}O$ measurements and used species-specific $\delta^{18}O$ paleotemperature equations to estimate their calcification depth (Meinicke et al., 2020). However, this approach cannot be applied to our polyspecific coccolith samples, because, as for planktic foraminifera (Spero et al., 2003), different species of coccolithophores feature significantly different $\delta^{18}O$ paleotemperature equations (Hermoso et al., 2015, 2014).

2.4.1. Selection of coccolithophores' main season of production

The production temperature of coccoliths at a given location is not precisely known because coccolithophores may calcify at a range of depths in the euphotic zone, and production may be concentrated in a particular season. Where limited by nutrients, for instance in areas of the subtropical and tropical oceans, productivity may be strongest during periods of de-stratification, a process which supplies nutrients and leads to cooler temperatures. On the other hand, where light is limiting, like at very high latitudes, primary producers generally show their highest biomass during warmest periods (Dandonneau et al., 2004).

We estimated the main season of production for each location from a variety of approaches. Where available, we relied on direct production estimates such as satellite-based chlorophyll *a* concentration and sediment trap coccolithophore fluxes. Additionally, we used oceanographic data obtained during cruises (e.g. using CTD stations) and floats, which elucidate the nutrient and physical controls on production, as well as models of production. The detailed information is provided in the Supplementary Note B and Supplementary Figs. B-E.

2.5. Construction of core top coccolith Δ_{47}-SST regression

We derive a core top coccolith Δ_{47}-SST regression with a similar approach as that used to establish the empirical calibration of the $U_{37}^{k'}$ thermometer, using SSTs (±1SE) of the season of production for each site (WOA, 2018), and our coccolith Δ_{47} measurements, and by applying the regression method of York et al. (2004).Click or tap here to enter text.Since this formulation does not consider the potential for coccolith calcification at depth, which could be significantly colder than at surface at some locations, this core top coccolith Δ_{47}-SST equation is not analogous to the Δ_{47} calibrations mentioned above (Anderson et al., 2021; Katz et al., 2017; Meinicke et al., 2021), and should therefore not be considered as a coccolith-specific calibration. However, we explore this approach for comparison to temperatures derived from core top $U_{37}^{k'}$-SST calibrations.

3. Results

3.1. Coccolith clumped and stable oxygen and carbon isotopes

Coccolith Δ_{47} decreases with increasing temperatures and ranges between 0.606 and 0.662 ‰ (I-CDES) (Table 1a, Fig. 2). These values are lower (warmer) and less variable than Δ_{47} values of globally-distributed core top foraminifera species, which vary between 0.653 and 0.756 ‰ (Meinicke et al., 2020) . Despite the inherent difficulties of comparing datasets generated using different standards, Δ_{47} and $\delta^{18}O$ values of the coccolithophore culture work of Katz et al. (2017), in which growth temperatures are similar to those we expect for our samples (7 to 25 °C), are similar in both magnitude and range of variation to our core top coccolith Δ_{47} and $\delta^{18}O$ values. Coccolith $\delta^{18}O$ varied by 5.5‰ (between -1.97 and 3.48 ‰, Table 1a, Fig. 2a).

Compared to $\delta^{18}O$, the range of variation of our coccolith $\delta^{13}C$ was smaller (from -0.01 to 1.36 ‰, Table 1a, Fig. 2b), except for one sample in the South Atlantic (3.03 ‰). Preindustrial $\delta^{13}C$ of dissolved inorganic carbon (DIC) in the surface ocean in regions represented by our core tops is simulated to vary spatially by less than 1.6‰ (Eide et al., 2017). Our core top samples therefore appear to manifest a smaller range of $\delta^{13}C$ vital effects (coccolith $\delta^{13}C$- $\delta^{13}C_{DIC}$) than observed among different species (5.7 ‰) in the culture study of Katz et al. (2017). Coccolith Δ_{47} and coccolith $\delta^{18}O$-$\delta^{18}O_{sw}$ show a significant positive correlation ($r = 0.84$, $p = 0.0007$; Fig. 2a). Since vital effects in coccolith $\delta^{13}C$ and $\delta^{18}O$ of a given species in cultures often correlate positively (e.g. Ziveri et al., 2003), as is the case for the cultures of Katz et al. (2017), a small vital effect in our coccolith $\delta^{13}C$ suggests likewise a small vital effect on $\delta^{18}O$.

Despite the relatively small inferred $\delta^{18}O$ vital effects in our dataset, calculating growth temperature and water depth habitats from coccolith $\delta^{18}O$ would not lead to more precise estimates. The variable oxygen isotope fractionations of different species and potential presence of environmental-driven variation in vital effects of a given species

(Hermoso et al., 2015, 2014) does not allow isolating temperature from vital effect influences in coccolith $\delta^{18}O$.

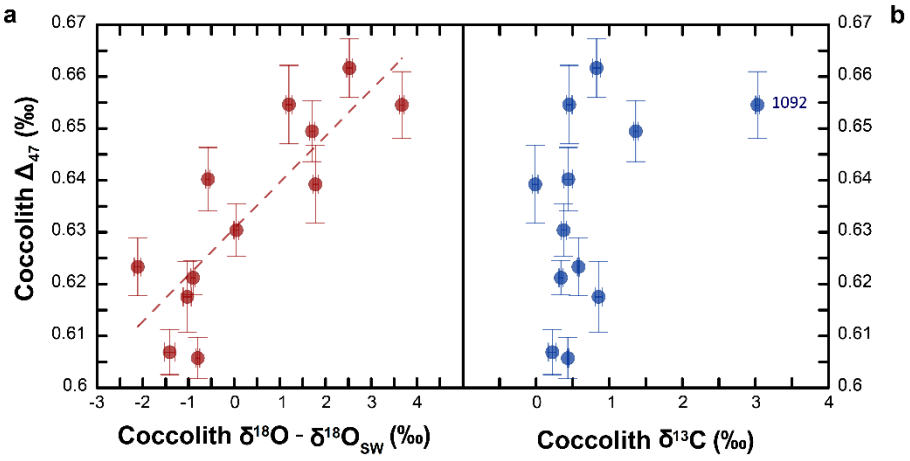

Fig. 2. Clumped isotopes (Δ_{47}, ‰) of coccolith separations as a function of **a)** coccolith $\delta^{18}O$ minus $\delta^{18}O$ of seawater ($\delta^{18}O$-$\delta^{18}O_{SW}$); where $\delta^{18}O$ of coccoliths is with respect to V-PDB and $\delta^{18}O_{SW}$ is with respect to V-SMOW, and **b)** coccolith $\delta^{13}C$. Seawater $\delta^{18}O$ used to calculate $\delta^{18}O$-$\delta^{18}O_{SW}$ are surface values from LeGrande and Schmidt (2006), and are similar to values to up to 50-100 m depth, depending on the Site. The positive correlation between coccolith Δ_{47} and $\delta^{18}O$ is statistically significant ($r = 0.84$, $p = 0.0007$). Error bars define one standard error of the Δ_{47} and one standard deviation of the $\delta^{18}O$ and $\delta^{13}C$.

3.2. SST during main season of production vs. $U^{k'}_{37}$ SST temperatures

Sea surface temperatures (0 m) WOA (2018) during the determined main season of peak production are reported in Table 1. For the tropical Equatorial Pacific locations, SSTs ranged from 20.9 to 25.8 °C, while those of the tropical oligotrophic sites were higher (26.6-27.5 °C). For the North Atlantic, peak production SSTs ranged from 14.5 °C at the mid-latitude IODP Site 1312 to 6.9 °C at our northernmost ODP Site 985. SSTs at

the South Atlantic and Southern Ocean locations varied from 17.5 °C (ODP Site 1266) to 4.1 °C (ODP Site 1093). $U_{37}^{k\prime}$ ratios varied between 0.330 and 0.965 (Table 1a), showing a clear latitudinal gradient. Although the calculated $U_{37}^{k\prime}$ temperature correlates with SSTs, regardless of the calibration used, $U_{37}^{k'}$ -derived temperatures (Table 1b) overestimate modern ocean SSTs of coccolithophore production season for most sites analyzed, with the largest differences generally observed at the highest latitudes and areas influenced by strong upwelling (Fig. 3, Supplementary Fig. F).

Table 1. a) Site, size fraction, ocean region, average and variation of the base of the mixed layer (MLD; m), and average SST (0 m, °C) during the season of production (Seas. Prod.), Δ_{47} value with standard error (‰) and number of replicates (n), alkenone unsaturation index ($U_{37}^{k'}$), and oxygen ($\delta^{18}O$) and carbon ($\delta^{13}C$) isotopic composition with standard deviation (‰, VPDB). SSTs and their respective standard deviations (SD) were obtained from WOA (2018). **b)** SST (°C) obtained using the core top[1] (Müller et al., 1998), bayspline[2] (Tierney and Tingley, 2018), and strain 55a *Emiliania huxleyi* batch culture[3] (Prahl et al., 1988) alkenone calibrations, calcification temperatures (CT; °C) obtained using the planktonic foraminifera[1] (Meinicke et al., 2021), the abiogenic[2] (Anderson et al., 2021), and the coccolithophore culture[3] (Katz et al., 2017) Δ_{47} calibrations, including uncertainties at the 95% CI, and average inferred habitat depth of coccolithophores (m) using the foraminifera Δ_{47} calibration to derive CT. * indicate Sites where including the 95% CI of estimated calcification temperatures, these are colder or warmer than SSTs during the season of production.

a

Site	Size fraction	Location	Seas. Prod.	MLD (m)	SST ± SD (°C)	Δ_{47} ± SE (‰)	n	$U^{k'}_{37}$	$\delta^{18}O$ ± SD (‰)	$\delta^{13}C$ ± SD (‰)
1093	<8	SO (Atl.)	Dec-Mar	69 (61-81)	4.12 ± 0.1	0.662 ± 0.006	12	0.330	2.27 ± 0.06	0.83 ± 0.06
1092	<8	SO (Atl.)	Nov-Feb	55 (49-65)	6.34 ± 0.1	0.655 ± 0.006	18		3.48 ± 0.05	3.03 ± 0.03
1122	<8	SO (West. Pac)	Dec-Jan	34 (32-36)	13.88 ± 0.1	0.655 ± 0.008	13	0.494	1.35 ± 0.06	0.45 ± 0.04
1266	<8	South Atlantic	Aug-Sep	78 (69-87)	17.46 ± 0.0	0.640 ± 0.006	17	0.691	0.10 ± 0.05	0.44 ± 0.06
1226	<8	Eq. Pacific	Aug-Sep	30 (28-31)	20.92 ± 0.2	0.621 ± 0.003	12	0.872	-0.61 ± 0.05	0.34 ± 0.03
U1338	<11	Eq. Pacific	Aug	29	24.67 ± 0.3	0.607 ± 0.004	11	0.965	-1.16 ± 0.11	0.22 ± 0.05
U1337	<11	Eq. Pacific	Aug	37	25.82 ± 0.0	0.606 ± 0.004	17	0.963	-0.54 ± 0.04	0.43 ± 0.01
1143	3-8	South China Sea	Dec-Mar	27 (25-31)	27.48 ± 0.2	0.623 ± 0.006	17	0.961	-1.97 ± 0.07	0.58 ± 0.01
999	<11	Colombian Car.	Jan-Mar	41 (40-42)	26.61 ± 0.1	0.618 ± 0.007	12		-0.25 ± 0.09	0.85 ± 0.05
U1312	<10	N. Atl. (Azores)	Apr-May	52 (36-69)	14.51 ± 0.3	0.630 ± 0.005	19	0.580	0.78 ± 0.05	0.38 ± 0.04
982	<10	N. Atl.	Dec-Jun	163 (29-261)	9.56 ± 0.3	0.649 ± 0.006	21	0.555	2.15 ± 0.06	1.36 ± 0.03
985	<10	N. Atl.	Jul	20	6.93 ± 0.6	0.639 ± 0.008	12	0.402	1.95 ± 0.06	-0.01 ± 0.04

b

Site	Location	SST ± SD (°C)	$U^{k'}_{37}$ SST^1 (°C)	$U^{k'}_{37}$ SST^2 (°C)	$U^{k'}_{37}$ SST^3 (°C)	$\Delta47$ CT^1 ± CI (95%) (°C)	$\Delta47$ CT^2 ± CI (95%) (°C)	$\Delta47$ CT^3 ± CI (95%) (°C)	Inferred depth (m)
1093	SO (Atl.)	4.12 ± 0.1	8.7	8.1	8.6	6.0 ± 3.4	1.8 ± 4.2	6.3 ± 4.3	0
1092	SO (Atl.)	6.34 ± 0.1				8.2 ± 3.8	4.5 ± 4.7	9.1 ± 4.9	0
1122	SO (West. Pac)	13.88 ± 0.1	13.6	12.9	13.4	8.1 ± 4.6	4.5 ± 5.7	9.1 ± 5.9	284*
1266	South Atlantic	17.46 ± 0.0	19.6	18.8	19.2	12.2 ± 3.9	9.6 ± 5.0	14.3 ± 5.2	292*
1226	Eq. Pacific	20.92 ± 0.2	25.1	24.6	24.5	17.7 ± 2.3	16.4 ± 2.9	21.4 ± 3.0	50
U1338	Eq. Pacific	24.67 ± 0.3	27.9	29.7	27.2	22.3 ± 3.0	22.3 ± 3.9	27.5 ± 4.0	61
U1337	Eq. Pacific	25.82 ± 0.0	27.8	29.2	27.2	22.7 ± 2.7	22.9 ± 3.6	28.1 ± 3.7	95
1143	South China Sea	27.48 ± 0.2	27.8	29.2	27.1	17.3 ± 3.6	15.9 ± 4.7	20.9 ± 4.8	152
999	Colombian Car.	26.61 ± 0.1				19.1 ± 4.7	18.3 ± 6.1	23.3 ± 6.3	179
U1312	N. Atl. (Azores)	14.51 ± 0.3	16.2	15.5	15.9	15.1 ± 3.2	13.1 ± 4.1	18.0 ± 4.2	0
982	N. Atl.	9.56 ± 0.3	15.5	15.0	15.2	9.6 ± 3.5	6.3 ± 4.3	10.9 ± 4.4	0
985	N. Atl.	6.93 ± 0.6	10.9	10.2	10.7	12.5 ± 4.8	9.9 ± 6.0	14.7 ± 6.2	0*

4. Discussion

As photosynthetic organisms, coccolithophores need to balance their supply of nutrients and light, and grazing pressure to grow (Arteaga et al., 2020; Behrenfeld et al., 2013; Mignot et al., 2018). Therefore, their preferred habitat depth depends on the ability of each species to achieve such a balance. Peak coccolithophore cell abundance is typically located right above the deep chlorophyll maximum (DCM), which coincides with the lower limit of the euphotic zone along a meridional transect in the Atlantic Ocean across temperate, subtropical gyres and equatorial regions (Balch et al., 2019; Poulton et al., 2017). Deeper than surface production also agrees with maximum coccolithophore concentrations at the South Pacific Gyre between 200-300 m (Beaufort et al., 2008) and in the tropical Indian Ocean (Liu et al., 2021). It remains to be solved whether these cells can grow with 10-1% of surface photosynthetic active radiation (PAR), or if they are senescent from surficial blooms. Our Δ_{47}-derived calcification temperatures provide new insights on this question because they give an indication of potential habitat depths in different oceanic settings.

4.1. Δ_{47} calibration used for estimating calcification temperatures

While considering the uncertainties of comparing temperature estimates derived from carbonate (Anderson et al., 2021; Meinicke et al., 2021) vs. gas (Katz et al., 2017) standardized Δ_{47} calibrations, the application of these calibrations to our coccolith Δ_{47} dataset does lead to up to 5.3 °C differences in calculated calcification temperatures (Table 1b). In general, the warmest temperatures are obtained with the calibration of Katz et al. (2017), while temperatures using the calibration of Anderson et al. (2021) are the

coldest (Table 1b). The mixed foraminifera calibration (Meinicke et al., 2021) overall leads to less extreme temperatures.

Continued improvements in analytical precision and interlaboratory comparability may evaluate if there are small, not yet detectable, vital effects in coccolith Δ_{47}. A more statistically robust coccolith-specific calibration could help to reduce uncertainties in the calculated temperatures from coccolith Δ_{47}. Given the current state of knowledge and absence of detected vital effects specific to coccolith biomineralization, we apply the recent foraminifera calibration of Meinicke et al. (2021) to our coccolith Δ_{47} for reasons detailed in section 2.3.4. In the following sections we discuss only temperatures derived from this calibration, while results derived from Anderson et al. (2021) and Katz et al. (2017) can be found in Table 1 and Supplementary Note C, Fig. G and H.

4.2. Coccolith Δ_{47}-derived calcification temperatures and coccolithophore's habitat depth

Coccolith Δ_{47} calcification temperatures show a clear latitudinal gradient (Fig. 3a). Except for ODP Site 985, Δ_{47}-derived temperatures are colder than temperatures obtained using $U_{37}^{k'}$ (Fig. 3c). Δ_{47} temperatures are either colder (low latitudes) or fall close to SSTs (mid-high latitudes). If the application of the foraminifera calibration (Meinicke et al., 2021) to our data is correct, and there is no significant additional vital effect in coccolith Δ_{47}, the calculated calcification temperatures indicate that coccolith calcification may take place within the euphotic zone but at a significant depth in some regions of the modern/Holocene ocean (Fig. 3b).

SEM observations do not show evidence of abiogenic carbonate overgrowth on coccoliths (Supplementary Note A, Fig. A). Moreover, Sr/Ca ratios of the analyzed fractions are consistent with those of coccolith calcite (e.g. Mejía et al., 2014, and refs.

479 therein), and exclude the presence of significant amounts of calcite precipitated from
480 seawater or pore fluids (Richter and Liang, 1993) in our samples (Supplementary Table
481 D). This suggests that fragments of unidentifiable origin are likely fragments from
482 coccoliths rather than authigenic carbonate. Therefore, the colder calcification
483 temperatures compared to SSTs of all our tropical Sites, and of ODP Sites 1122 and 1266,
484 are likely not a consequence of diagenetic alteration. Although some tropical samples
485 included subeuphotic zone coccolith species like *F. profunda* and *Ceratholitus cristatus,*
486 the contribution of subeuphotic carbonate is less than 17% (Supplementary Figure I).
487 Therefore, the potential cold signal introduced by their presence cannot explain by itself
488 the large magnitude of difference between SSTs and coccolith Δ_{47}-derived temperatures
489 (e.g. 7.5 °C for Site 999) (Supplementary Note D).

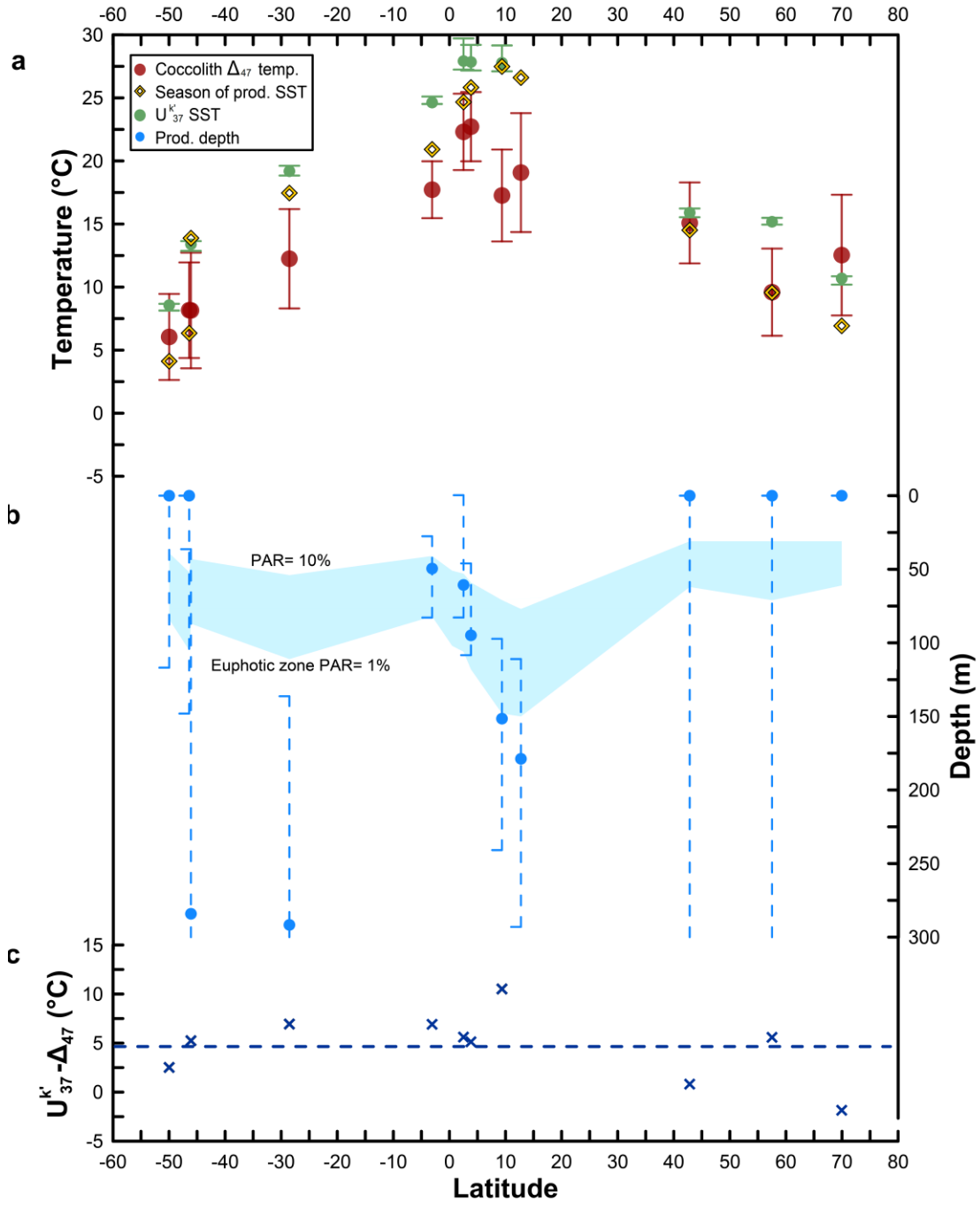

Fig. 3. a) Calcification temperatures (±95% CI) from coccolith Δ_{47} calculated with the foraminifera calibration (Meinicke et al., 2021) (red circles), SSTs from $U^{k\prime}_{37}$ (green circles), and average WOA SSTs during peak production months (yellow diamonds). $U^{k\prime}_{37}$ SSTs were estimated using the core top (Müller et al., 1998), bayspline (Tierney and Tingley, 2018), and the 55a *Emiliania huxleyi* batch culture (Prahl et al., 1988) calibrations, and error bars denote the maximum and minimum SST values. **b)** Coccolithophore habitat depths inferred from coccolith Δ_{47} calcification temperatures. Error bars indicating the potential shallowest and deepest habitat depths are calculated

using the warmest and coldest Δ_{47}-temperatures from the 95% CI extremes. Open error bars denote a > 300 m depth limit. Depths below the euphotic zone are unrealistic. The blue shaded area denotes depths where PAR ranges between 10-1%. **c)** Difference between $U_{37}^{k\prime}$-annual SSTs and coccolith Δ_{47}-temperatures (blue cross). This calculation considers $U_{37}^{k\prime}$ -SSTs estimated using the calibration that leads to medium values compared to the other two calibrations. Blue dashed line shows that on average $U_{37}^{k\prime}$-annual SSTs are 4.7 °C warmer than coccolith Δ_{47}-temperatures.

4.2.1. Tropical Pacific upwelling and tropical oligotrophic ocean regions

Phytoplankton is recognized to grow throughout the euphotic zone (Behrenfeld et al., 2013). The 2.4-3.2 °C and the 7.5-10.2 °C colder coccolith Δ_{47} calcification temperatures compared to SSTs during the season of production at tropical upwelling and tropical oligotrophic sites (Fig. 3a), respectively, are consistent with a deeper than surface habitat in these regions (Fig. 3b; Table 1). In tropical regions with a strong thermocline and a shallow mixed layer, the abundance of placolith-bearing coccolithophores, including alkenone producers, has been shown to peak well below the surface. In the South Pacific gyre, highest cell abundances are found at 200 m depth (Beaufort et al., 2008), while in northern and southern oligotrophic regions of the Atlantic and in the Equatorial Atlantic, peaks in coccosphere abundance follow a ~45 m thick layer just above the DCM (1% PAR; lower limit of euphotic zone) (Poulton et al., 2017). This habitat distribution is likely a consequence of nutrient depletion in the surface layers, combined with the ability of most coccolithophores to obtain enough light at depths just above the lower limit of the euphotic zone. Our coccolith Δ_{47}-calcification temperatures from all tropical sites are consistent with the hypothesis that coccospheres and coccoliths retrieved at depth (e.g. Beaufort et al., 2008; Cortés et al., 2001; Poulton et al., 2017) are not senescent cells, but are rather actively growing and calcifying cells adapted to low light conditions.

Coccolith Δ_{47}-calcification temperatures in all Equatorial Pacific Sites (IODP U1337, U1338 and ODP 1226) suggest that coccolithophore habitats are located above the lower limit of the euphotic zone, but well below the surface, at depths between 50-95 m (Table 1b). Inferred habitat depths from Equatorial Pacific coccolith Δ_{47} temperatures agree within error with depths where light levels fall between 10 and 1% PAR (average values ranging from 14 to 41 $\mu E\ m^{-2}\ s^{-1}$) (Fig. 3b, Fig. 4a, b, c), which is consistent with highest coccosphere abundance and diversity of low euphotic zone species in Equatorial regions (Poulton et al., 2017).

Considering the relatively large uncertainties in coccolith Δ_{47}-temperatures of both oligotrophic tropical sites (ODP 999: ± 4.7°C and 1143: ± 3.6 °C), and that especially for Site 999, the $CaCO_3$ contribution of the subeuphotic species *F. profunda* (~17%) is expected to have introduced a cold bias in calcification temperatures (Supplementary Note D, Supplementary Fig. I), coccolith Δ_{47}-inferred habitat depths also agree within error with depths where light levels vary between 10% and 1% (Fig. 3b, Fig. 4d, e). Δ_{47}-calcification temperatures at Sites 999 and 1143 would be expected to suggest deeper habitats, closer to the lower limit of the euphotic zone at ~150 m, compared to the more productive Equatorial Pacific regions (from 50-95 m). These observations are consistent with deeper coccosphere abundance peaks in oligotrophic regions (~140 m) vs. Equatorial areas (~70 m) of the Atlantic (Poulton et al., 2017).

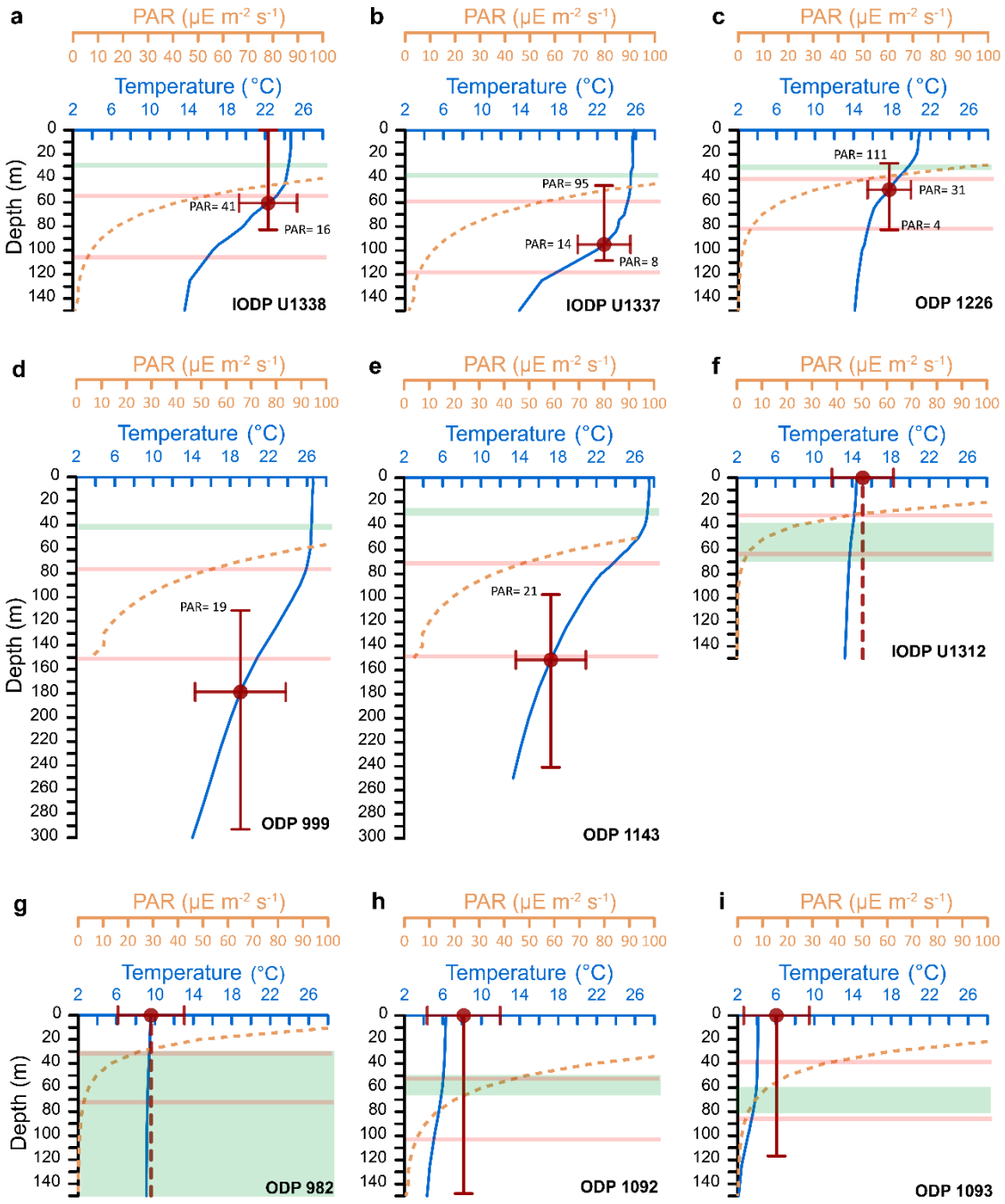

Fig. 4. Vertical temperature profile (solid blue line) and photosynthetic active radiation (PAR; dashed orange line) at our sites. Coccolith Δ_{47}-calcification temperatures (red circles) locate the likely habitat depth of coccolithophores. Horizontal error bars indicate the possible range of calcification temperature variation (95% CI). We use these warmest and coldest calcification temperatures to determine the potential shallowest and deepest habitat, respectively, here denoted by vertical error bars. Dashed vertical error bars indicate a potential habitat depth outside the depth scale in the y axis. The green shaded area indicates the variation of the base of the mixed layer during the peak production

months. Horizontal red lines comprise the depth where PAR varies between 10 and 1% (limit of euphotic zone), below which coccolithophores are likely not living.

4.2.2. High latitudes in the North and South Atlantic and the Southern Ocean

At IODP Site U1312 and ODP Sites 982, 1092 and 1093, coccolith Δ_{47} calcification temperatures agree within error with SSTs, suggesting a rather surficial production (Fig. 3, Fig. 4f-i). At higher latitudes, where the mixed layer is deeper than in low latitudes, light availability is often more limited than nutrients (Dandonneau et al., 2004), potentially forcing coccolithophores to remain closer to the surface. Given the relatively large analytical uncertainty of clumped isotope thermometry, and the small vertical temperature gradient typical of high latitudes, the attribution of a specific habitat depth in these settings is less accurate compared to more stratified areas.

From the analysis of calcification temperatures and habitat depths of our tropical locations, we conclude that PAR levels as low as 14 $\mu E\ m^{-2}\ s^{-1}$ can sustain coccolithophore production. Therefore, it is possible that high latitude coccolithophores can also thrive under much lower than surface PAR levels (238-542 $\mu E\ m^{-2}\ s^{-1}$ at our high latitude sites during season of production). Requirement of rather low PAR levels for coccolithophore production at high latitudes agree with the average mixed layer PAR levels (~1.5-12 $E\ m^{-2}\ d^{-1}$, i.e. ~17-138 $\mu E\ m^{-2}\ s^{-1}$) reported for the Southern Ocean phytoplankton blooming phase using extensive float data (Arteaga et al., 2020). Given the lack of motility during their diploid phase, calcification of heterococcoliths in these sites is therefore likely occurring throughout the mixed layer and not exclusively at the very surface. This hypothesis also agrees with the larger overlap of irradiance levels in which lower photic zone coccolithophore species from temperate zones are observed (Poulton et al., 2017). Consequently, we suggest that coccolith Δ_{47} from well-mixed high latitudes are a good indicator of mixed layer temperatures during the season of coccolithophore production.

Coccolith Δ_{47} temperatures at ODP Sites 1266 in the Walvis Ridge and 1122 in the Pacific Sector of the Southern Ocean are 5.2 and 5.7 °C colder than SSTs during the season of production, respectively. Such large differences, at places with a small thermocline, result in unrealistic calculated habitat depth ranges, well below the euphotic zone, where coccolithophores cannot photosynthesize (Fig. 4b, Supplementary Fig. J). While ODP Site 1266 can be influenced by the Benguela upwelling system, especially during winters, as filaments can extend up to 1000 km from the upwelling foci (Romero et al., 2002), not even a total contribution of advected coccoliths from upwelling locations can explain the cold Δ_{47} temperatures. With the available data, we cannot explain the calcification temperature biases for these two Sites.

The North Atlantic highest latitude ODP Site 985, in contrast, show average coccolith Δ_{47} temperatures 5.6 °C warmer than the season of production SSTs (Supplementary Fig. J). This could be explained if, for instance, the preserved and analyzed coccoliths were disproportionately produced during years with temperatures far warmer than those of the modern ocean's season of production (e.g heat wave years).

5. Implications for paleotemperature reconstructions

If the commonly used temperature proxies all recorded surface ocean conditions, as is commonly assumed, then they should also yield similar absolute values. In principle, this assumption would be even more valid if proxies are phytoplankton-based, given their light requirement for photosynthesis. If the habitat of placolith-bearing coccolithophores, including alkenone producers, was invariably surficial geographically and temporally, $U_{37}^{k'}$ and coccolith Δ_{47}-derived temperatures would be expected to show matching absolute values corresponding to SSTs, since alkenones and coccolith $CaCO_3$ are both

produced by coccolithophores, and the $U_{37}^{k'}$ proxy is calibrated to SSTs (Müller et al., 1998; Tierney and Tingley, 2018).

The comparison of $U_{37}^{k'}$ and coccolith Δ_{47} in the core tops shows that Δ_{47} calcification temperatures estimated using Meinicke et al. (2021) are on average 4.7 °C colder than SSTs recorded by the $U_{37}^{k'}$ proxy. One explanation is that coccolithophores are not growing and calcifying at the surface in all oceanographic settings. In our dataset, $U_{37}^{k'}$-derived temperatures are generally higher than measured SSTs during the season of coccolithophore production (Fig. 3a, Supplementary Fig. F). On the other hand, Δ_{47} calcification temperatures are colder than SSTs in tropical regions, which is consistent with a deeper than surface production (Fig. 3b). This difference needs to be accounted for in inter-proxy comparisons of coccolith Δ_{47} temperatures with proxies regressed to SST.

5.1. Core top coccolith Δ_{47}-SST regression

The most widely applied core top calibrations do not relate $U_{37}^{k'}$ to actual alkenone production temperature, but rather to SST (Müller et al., 1998; Tierney and Tingley, 2018). We follow the same approach and calculate a core top coccolith Δ_{47}-SST regression (Fig. 5a) to facilitate comparison of coccolith Δ_{47} calcification temperatures with SST-regressed proxies like $U_{37}^{k'}$. The application of a York et al. (2004) regression across all samples defines the following equation between coccolith Δ_{47} and average WOA SSTs during peak production months:

$$\Delta_{47}\text{ (I-CDES 90°C)} = 0.0261 \pm 0.0024 * 10^6/\text{SST}^2 + 0.3198 \pm 0.0280 \text{ (SST in K)} \quad (1)$$

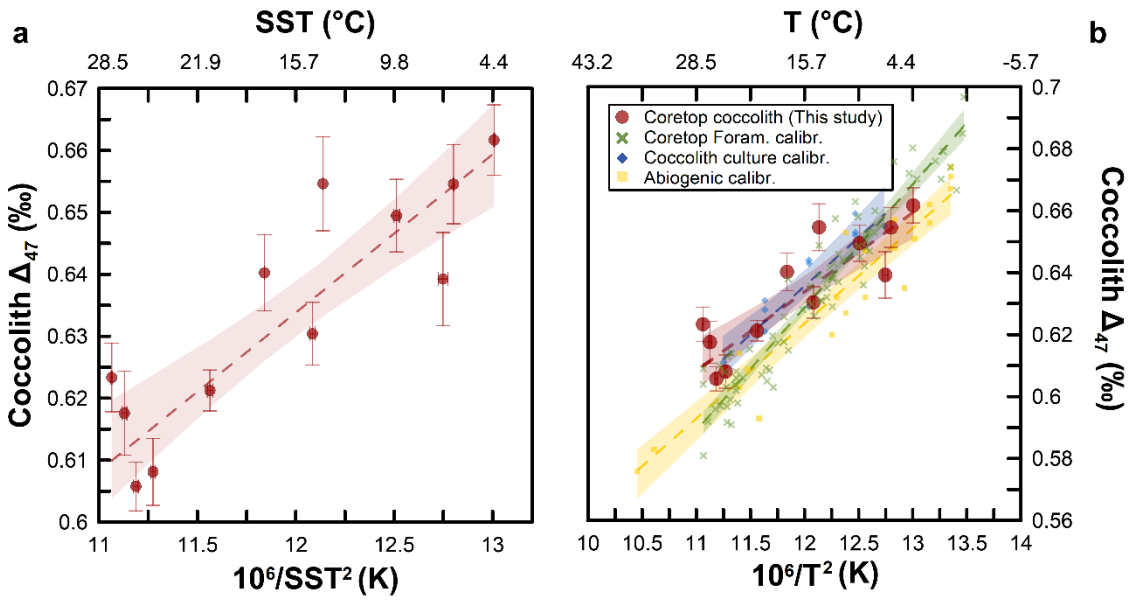

Fig. 5. a) Clumped isotopes (Δ_{47}, ‰) of our coccolith core top separations as a function of SST during the season of production, expressed both as $10^6/SST^2$ (SST in K), and as °C. Dashed red line represent the core top coccolith Δ_{47} regression, red shaded area represents the 95% CI. **b),** core top coccolith Δ_{47} regression (dashed red line, n=12) plotted together with the Anderson et al. (2021) (dashed yellow line, n=23), the Katz et al. (2017) (dashed blue line, n=11), and the Meinicke et al. (2021) calibrations (dashed green line, n=78), all obtained using the York et al. (2004) method. Shaded areas represent the 95% CI of the regressions. Vertical error bars represent 1SE of the Δ_{47} measurements, and horizontal error bars represent the average SE of the SSTs of the production months.

Our core top coccolith Δ_{47} show a strong and significant inverse correlation to average WOA SSTs ($r = 0.8751$; $p < 0.001$) (Fig 5a, Table 2). If coccolithophores were calcifying at depth rather than at the surface, a strong Δ_{47}-SST correlation can still arise because of the correlation between SSTs and temperatures at their habitat's depth.

Table 2. Regression of coccolith core top Δ_{47}-SST during season of production compared to recent Δ_{47} calibrations, including slope, intercept, and respective standard errors, all expressed in the I-CDES 90°C reference frame. The abiogenic (Anderson et al., 2021) and the coccolithophore culture (Katz et al., 2017) calibrations use experimental (Exp.) growth temperatures, while the planktonic foraminifera calibration (Coretop Foram) uses

inferred (Inf)/calculated *in situ* temperatures, not necessarily from the surface (Meinicke et al., 2021). Standardization and data correction in the study of Katz et al. (2017) did not follow the same methodology as applied for other studies, including ours, introducing uncertainty in comparability between calibrations. Here we only consider data from the Anderson et al. (2021) calibration in the range of temperature relevant for coccolithophore environments (< 36.1 °C).

Regression (R)/Calibration (C)	Temp.	Slope±SE	Intercept±SE	r
R Coretop coccolith (this study)	SST	0.0261±0.0024	0.3198±0.0280	0.8751
C Coretop Foram. (Meinicke et al., 2021)	Inf. *in situ*	0.0397±0.0011	0.1518±0.0128	0.9174
C Culture (Katz et al., 2017)	Exp.	0.0313±0.0028	0.2602±0.0339	0.9410
C Abiogenic <36.1°C (Anderson et al., 2021)	Exp.	0.0307±0.0035	0.2549±0.0422	0.9521

ANCOVA analyses show that the slope and the intercept of our coccolith Δ_{47} regression are not statistically different from those of Anderson et al. (2021) (p_{slope} = 0.11; $p_{intercept}$ = 0.08; data <40 °C), while they are different to the those of the foraminifera calibration (Meinicke et al., 2021; p_{slope} < 0.005; $p_{intercept}$ < 0.005) (Supplementary Table E). Even if not statistically different to the abiotic calibration, the slope of the coccolith Δ_{47}-SST regression is shallower compared to the theoretical value and all mentioned Δ_{47} calibrations (Fig. 5b; Table 2). This shallower slope is especially influenced by a few warm samples, thus supporting the notion that especially at tropical sites coccoliths have deeper and cooler habitats. This can explain the larger offset between SST and Δ_{47} calcification temperatures at lower warmer latitudes than at colder higher ones. A shallower slope and a slight mismatch between our coccolith Δ_{47}-SST regression and other published Δ_{47} calibrations would be a further argument for a deeper than surface coccolith calcification in some ocean settings, as temperatures from other calibrations are either experimental or inferred *in situ.* Conversely, our regression uses SSTs, regardless if they match or not actual calcification temperatures.

Because the coccolith Δ_{47}-SST regression does not account for the potential for calcification at depth, we emphasize that it should be not used to calculate SSTs. It could be rather used as a tool to compare to SST-regressed proxies (like $U_{37}^{k'}$) in future studies, taking into account that this approach would lead to overestimation of absolute temperatures of production. Further work on both proxies is required to improve absolute temperature reconstructions and resolve the implication of production depth on estimation of SST.

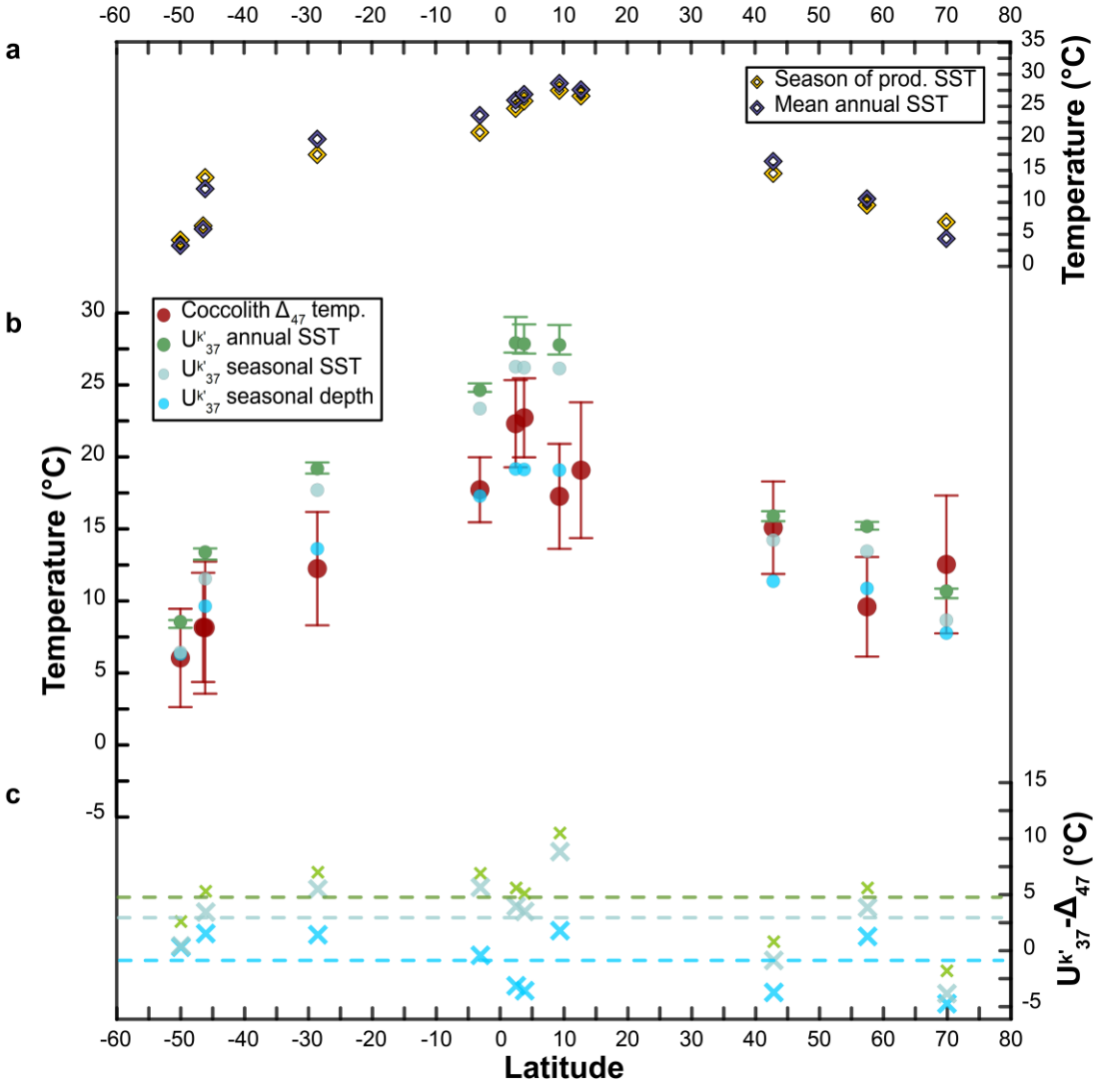

Fig. 6. a) Mean annual SSTs (deep blue diamonds) and SSTs during peak production months (yellow diamonds). **b)** Calcification temperatures (±95% CI) from coccolith Δ_{47} calculated with the foraminifera calibration (Meinicke et al., 2021) (red circles); mean

annual SSTs (green circles) applying published (Müller et al., 1998; Prahl et al., 1988; Tierney and Tingley, 2018) $U_{37}^{k'}$ calibrations to our $U_{37}^{k'}$; seasonal SSTs (blue-green circles) applying an independent $U_{37}^{k'}$-seasonal SST regression to our $U_{37}^{k'}$, which is based on a subset of sites of the study of Tierney and Tingley (2018), which coincide geographically with our locations; and seasonal temperatures at depth of production (light blue circles) applying an independent $U_{37}^{k'}$-seasonal depth temperature regression to our $U_{37}^{k'}$, based on the same subset of sites from Tierney and Tingley (2018), and considering habitat depths inferred from our coccolith Δ_{47} database. **c)** Difference between $U_{37}^{k'}$-annual SSTs (green cross, average difference 4.7 °C), $U_{37}^{k'}$ seasonal SSTs (blue-green crosses, average difference 3.0 °C), and $U_{37}^{k'}$ seasonal deep temperatures (light blue crosses, average difference -0.9 °C) and coccolith Δ_{47}-calcification temperatures (Meinicke et al., 2021).

5.2. Snapshot into alternative alkenone calibrations: are alkenones also produced at depth?

We compare the relationship between $U_{37}^{k'}$ and seasonal SSTs (rather than annual) and to subsurface temperatures. For this, we selected an independent sample set, a subset of sites from the alkenone calibration work of Tierney and Tingley (2018), which are proximal to our sites and for which we apply similar season and habitat of production. For this independent sample subset, we then calculated alternative $U_{37}^{k'}$ calibrations using: a) SSTs during the season of production, and b) temperatures at the depth and season of production inferred for that oceanic setting from our coccolith Δ_{47} dataset (Fig. 6 d, e, Supplementary Note E and Fig. K). We propose that alternative $U_{37}^{k'}$ calibrations considering seasonal temperatures of calcification and alkenone production at depth with a large $U_{37}^{k'}$ dataset could improve the robustness and coherency of paleotemperature estimates.

6. Conclusions

Coccoliths from globally distributed core top sediments show promise for Δ_{47} thermometry, since Δ_{47} correlates with sea surface temperatures during the production season and also correlates with the temperature component of $\delta^{18}O$ variation in coccoliths ($\delta^{18}O_{calcite}$- $\delta^{18}O_w$). Application of the statistically-robust and carbonate-standardized foraminifera Δ_{47} calibration, the most appropriate available calibration for biogenic carbonate, yields coccolith calcification temperatures colder than SSTs for all tropical locations. This suggests that coccolithophores at these locations likely live at depth and can thrive with PAR levels between 1-10%. For well-mixed high latitudes, coccolith Δ_{47} calcification temperatures likely reflect mixed layer temperatures.

Because phytoplankton's ability to accumulate cells in the ocean depends on a complex conjunction of forcing factors, their actual habitat may not obey the convenient simplifications historically used for calibration of their temperature proxies. Future studies will determine if the use of a statistically well-constrained coccolith Δ_{47} calibration could further reduce uncertainties in estimated absolute calcification temperatures and habitat depths. Potentially, coccolith Δ_{47} combined with concurrent analysis of planktic foraminifera occupying different depths, could be used to add constraints on the vertical thermal structure of the photic zone.

If further work substantiates the evidence here for significant deep photic zone production by alkenone-producing coccolithophores in some (or all) oceanic settings, the convention of regressing the $U^{k'}_{37}$ parameter to surface ocean temperature may need reassessment to account for the spatially (and potentially temporally) variable relationship between production and surface temperatures. The assignment of absolute temperatures to their correct depth would allow climate models to compare their outputs with more accurate datasets, improving their reliability.

Author contributions

L.M.M and H.Z developed the separation method; A.F developed the cleaning method; L.M.M separated and cleaned the coccoliths, and with M.J measured clumped isotopes under the direction of S.B; L.M.M and M.J prepared and measured samples for trace element analysis. L.M.M took the SEM pictures; H.Z. evaluated coccolith assemblages. L.M.M purified alkenones and L.M.M and J.G. measured alkenones. I.H.A helped with data acquisition. N.H measured radiocarbon. The study was conceived by L.M.M, H.S and S.B. L.M.M wrote the paper with contributions from H.S and S.B.

Declaration of competing interests

There are no competing interests.

Acknowledgements

This project has received funding from the European Union's Horizon 2020 research and innovation programme under the Marie Sklodowska-Curie grant agreement 795053, from the Cluster of Excellence (RECORDER unit) of MARUM, from ETH Zurich Core funding, and Swiss National Science Foundation (Award 200021_182070). We thank Jakub Sliwinski for assistance during SEM analysis, Niklas Meinicke for assistance with data processing, and laboratory assistant Thierry Solms for helping to purify alkenones.

Additional information

Supplementary information is available in the online version of the paper.

References

Agterhuis, T., Ziegler, M., de Winter, N.J., Lourens, L.J., 2022. Warm deep-sea temperatures across Eocene Thermal Maximum 2 from clumped isotope thermometry. Communications Earth & Environment 2022 3:1 3, 1–9. https://doi.org/10.1038/s43247-022-00350-8

Anderson, N.T., Kelson, J.R., Kele, S., Daëron, M., Bonifacie, M., Horita, J., Mackey, T.J., John, C.M., Kluge, T., Petschnig, P., Jost, A.B., Huntington, K.W., Bernasconi, S.M., Bergmann, K.D., 2021. A Unified Clumped Isotope Thermometer Calibration (0.5–1,100°C) Using Carbonate-Based Standardization. Geophys Res Lett 48, e2020GL092069. https://doi.org/10.1029/2020GL092069

Arteaga, L.A., Boss, E., Behrenfeld, M.J., Westberry, T.K., Sarmiento, J.L., 2020. Seasonal modulation of phytoplankton biomass in the Southern Ocean. Nature Communications 2020 11:1 11, 1–10. https://doi.org/10.1038/s41467-020-19157-2

Balch, W.M., Bowler, B.C., Drapeau, D.T., Lubelczyk, L.C., Lyczkowski, E., Mitchell, C., Wyeth, A., 2019. Coccolithophore distributions of the North and South Atlantic Ocean. Deep Sea Research Part I: Oceanographic Research Papers 151, 103066. https://doi.org/10.1016/J.DSR.2019.06.012

Beaufort, L., Couapel, M., Buchet, N., Claustre, H., Goyet, C., 2008. Calcite production by coccolithophores in the south east Pacific Ocean. Biogeosciences 5, 1101–1117. https://doi.org/10.5194/bg-5-1101-2008

Behrenfeld, M.J., Doney, S.C., Lima, I., Boss, E.S., Siegel, D.A., 2013. Annual cycles of ecological disturbance and recovery underlying the subarctic Atlantic spring plankton bloom. Global Biogeochem Cycles 27, 526–540. https://doi.org/10.1002/gbc.20050

Bernasconi, S.M., Daëron, M., Bergmann, K.D., Bonifacie, M., Meckler, A.N., Affek, H.P., Anderson, N., Bajnai, D., Barkan, E., Beverly, E., Blamart, D., Burgener, L., Calmels, D., Chaduteau, C., Clog, M., Davidheiser-Kroll, B., Davies, A., Dux, F., Eiler, J., Elliott, B., Fetrow, A.C., Fiebig, J., Goldberg, S., Hermoso, M., Huntington, K.W., Hyland, E., Ingalls, M., Jaggi, M., John, C.M., Jost, A.B., Katz, S., Kelson, J., Kluge, T., Kocken, I.J., Laskar, A., Leutert, T.J., Liang, D., Lucarelli, J., Mackey, T.J., Mangenot, X., Meinicke, N., Modestou, S.E., Müller, I.A., Murray, S., Neary, A., Packard, N., Passey, B.H., Pelletier, E., Petersen, S., Piasecki, A., Schauer, A., Snell, K.E., Swart, P.K., Tripati, A., Upadhyay, D., Vennemann, T., Winkelstern, I., Yarian, D., Yoshida, N., Zhang, N., Ziegler, M., 2021. InterCarb: A Community Effort to Improve Interlaboratory Standardization of the Carbonate Clumped Isotope Thermometer Using Carbonate Standards. Geochemistry, Geophysics, Geosystems 22, e2020GC009588. https://doi.org/10.1029/2020GC009588

Bouchard', J.N., Roy, S., Campbell', D.A., 2006. UVB Effects on the Photosystem II-D1 Protein of Phytoplankton and Natural Phytoplankton Communities. Photochem Photobiol 82, 936–951. https://doi.org/10.1562/2005-08-31-IR-666

Caldarescu, D.E., Sadatzki, H., Andersson, C., Schäfer, P., Fortunato, H., Meckler, A.N., 2021. Clumped isotope thermometry in bivalve shells: A tool for reconstructing seasonal upwelling. Geochim Cosmochim Acta 294, 174–191. https://doi.org/10.1016/J.GCA.2020.11.019

Cortés, M.Y., Bollmann, J., Thierstein, H.R., 2001. Coccolithophore ecology at the HOT station ALOHA, Hawaii. Deep Sea Res 2 Top Stud Oceanogr 48, 1957–1981. https://doi.org/10.1016/S0967-0645(00)00165-X

807 Dandonneau, Y., Deschamps, P.Y., Nicolas, J.M., Loisel, H., Blanchot, J., Montel, Y.,
808 Thieuleux, F., Bécu, G., 2004. Seasonal and interannual variability of ocean color
809 and composition of phytoplankton communities in the North Atlantic, equatorial
810 Pacific and South Pacific. Deep Sea Research Part II: Topical Studies in
811 Oceanography 51, 303–318. https://doi.org/10.1016/J.DSR2.2003.07.018
812 Drury, A.J., John, C.M., 2016. Exploring the potential of clumped isotope thermometry
813 on coccolith-rich sediments as a sea surface temperature proxy. Geochemistry,
814 Geophysics, Geosystems 17, 4092–4104. https://doi.org/10.1002/2016GC006459
815 Dudley, W.C., Blackwelder, P., Brand, L., Duplessy, J.C., 1986. Stable isotopic
816 composition of coccoliths. Mar Micropaleontol 10, 1–8.
817 https://doi.org/10.1016/0377-8398(86)90021-6
818 Eide, M., Olsen, A., Ninnemann, U.S., Johannessen, T., 2017. A global ocean
819 climatology of preindustrial and modern ocean δ13C. Global Biogeochem Cycles
820 31, 515–534. https://doi.org/10.1002/2016GB005473
821 Eiler, J.M., 2011. Paleoclimate reconstruction using carbonate clumped isotope
822 thermometry. Quat Sci Rev 30, 3575–3588.
823 https://doi.org/10.1016/j.quascirev.2011.09.001
824 Eiler, J.M., 2007. “Clumped-isotope” geochemistry-The study of naturally-occurring,
825 multiply-substituted isotopologues. Earth Planet Sci Lett 262, 309–327.
826 https://doi.org/10.1016/j.epsl.2007.08.020
827 Evans, D., Sagoo, N., Renema, W., Cotton, L.J., Müller, W., Todd, J.A., Saraswati,
828 P.K., Stassen, P., Ziegler, M., Pearson, P.N., Valdes, P.J., Affek, H.P., 2018.
829 Eocene greenhouse climate revealed by coupled clumped isotope-Mg/Ca
830 thermometry. Proc Natl Acad Sci U S A 115, 1174–1179.
831 https://doi.org/10.1073/PNAS.1714744115/SUPPL_FILE/PNAS.1714744115.SD0
832 2.XLSX
833 Fernandez, A., Müller, I.A., Rodríguez-Sanz, L., Dijk, J. van, Looser, N., Bernasconi,
834 S.M., 2017. A Reassessment of the Precision of Carbonate Clumped Isotope
835 Measurements: Implications for Calibrations and Paleoclimate Reconstructions.
836 Geochemistry, Geophysics, Geosystems 18, 4375–4386.
837 https://doi.org/10.1002/2017GC007106@10.1002/(ISSN)1525-2027.ISOTOPE1
838 Fiebig, J., Daëron, M., Bernecker, M., Guo, W., Schneider, G., Boch, R., Bernasconi,
839 S.M., Jautzy, J., Dietzel, M., 2021. Calibration of the dual clumped isotope
840 thermometer for carbonates. Geochim Cosmochim Acta 312, 235–256.
841 https://doi.org/10.1016/J.GCA.2021.07.012
842 Ghosh, P., Adkins, J., Affek, H., Balta, B., Guo, W., Schauble, E.A., Schrag, D., Eiler,
843 J.M., 2006. 13C-18O bonds in carbonate minerals: A new kind of
844 paleothermometer. Geochim Cosmochim Acta 70, 1439–1456.
845 https://doi.org/10.1016/j.gca.2005.11.014
846 Guan, W., Gao, K., 2010. Impacts of UV radiation on photosynthesis and growth of the
847 coccolithophore Emiliania huxleyi (Haptophyceae). Environ Exp Bot 67, 502–508.
848 https://doi.org/10.1016/J.ENVEXPBOT.2009.08.003
849 Guitián, J., Stoll, H.M., 2021. Evolution of Sea Surface Temperature in the Southern
850 Mid-latitudes From Late Oligocene Through Early Miocene. Paleoceanogr
851 Paleoclimatol 36, e2020PA004199. https://doi.org/10.1029/2020PA004199
852 Hermoso, M., Candelier, Y., Browning, T.J., Minoletti, F., 2015. Environmental control
853 of the isotopic composition of subfossil coccolith calcite: Are laboratory culture
854 data transferable to the natural environment? GeoResJ 7, 35–42.
855 https://doi.org/10.1016/J.GRJ.2015.05.002

Hermoso, M., Horner, T.J., Minoletti, F., Rickaby, R.E.M., 2014. Constraints on the vital effect in coccolithophore and dinoflagellate calcite by oxygen isotopic modification of seawater. Geochim Cosmochim Acta 141, 612–627. https://doi.org/10.1016/J.GCA.2014.05.002

Ho, S.L., Laepple, T., 2016. Flat meridional temperature gradient in the early Eocene in the subsurface rather than surface ocean. Nat Geosci 9, 606–610. https://doi.org/10.1038/ngeo2763

John, C.M., Bowen, D., 2016. Community software for challenging isotope analysis: First applications of 'Easotope' to clumped isotopes. Rapid Communications in Mass Spectrometry 30, 2285–2300. https://doi.org/10.1002/rcm.7720

Katz, A., Bonifacie, M., Hermoso, M., Cartigny, P., Calmels, D., 2017. Laboratory-grown coccoliths exhibit no vital effect in clumped isotope (Δ47) composition on a range of geologically relevant temperatures. Geochim Cosmochim Acta 208, 335–353. https://doi.org/10.1016/j.gca.2017.02.025

Kretschmer, K., Jonkers, L., Kucera, M., Schulz, M., 2018. Modeling seasonal and vertical habitats of planktonic foraminifera on a global scale. Biogeosciences 15, 4405–4429. https://doi.org/10.5194/BG-15-4405-2018

LeGrande, A.N., Schmidt, G.A., 2006. Global gridded data set of the oxygen isotopic composition in seawater. Geophys Res Lett 33, 12604. https://doi.org/10.1029/2006GL026011

Leutert, T.J., Auderset, A., Martínez-García, A., Modestou, S., Meckler, A.N., 2020. Coupled Southern Ocean cooling and Antarctic ice sheet expansion during the middle Miocene. Nature Geoscience 2020 13:9 13, 634–639. https://doi.org/10.1038/s41561-020-0623-0

Leutert, T.J., Modestou, S., Bernasconi, S.M., Meckler, A.N., 2021. Southern ocean bottom-water cooling and ice sheet expansion during the middle Miocene climate transition. Climate of the Past 17, 2255–2271. https://doi.org/10.5194/CP-17-2255-2021

Liu, H., Wang, D., Yun, M., Zhang, X., Zhang, G., Thangaraj, S., Sun, J., 2021. Vertical Biogeography and Realized Niche Traits of Living Coccolithophore Community in the Eastern Indian Ocean. J Geophys Res Biogeosci 126, e2020JG005922. https://doi.org/10.1029/2020JG005922

Lunt, D.J., Bragg, F., Chan, W. le, Hutchinson, D.K., Ladant, J.B., Morozova, P., Niezgodzki, I., Steinig, S., Zhang, Z., Zhu, J., Abe-Ouchi, A., Anagnostou, E., de Boer, A.M., Coxall, H.K., Donnadieu, Y., Foster, G., Inglis, G.N., Knorr, G., Langebroek, P.M., Lear, C.H., Lohmann, G., Poulsen, C.J., Sepulchre, P., Tierney, J.E., Valdes, P.J., Volodin, E.M., Dunkley Jones, T., Hollis, C.J., Huber, M., Otto-Bliesner, B.L., 2021. DeepMIP: Model intercomparison of early Eocene climatic optimum (EECO) large-scale climate features and comparison with proxy data. Climate of the Past 17, 203–227. https://doi.org/10.5194/CP-17-203-2021

McIntyre, C.P., Wacker, L., Haghipour, N., Blattmann, T.M., Fahrni, S., Usman, M., Eglinton, T.I., Synal, H.A., 2017. Online 13C and 14C Gas Measurements by EA-IRMS–AMS at ETH Zürich. Radiocarbon 59, 893–903. https://doi.org/10.1017/RDC.2016.68

Meckler, A.N., Sexton, P.F., Piasecki, A.M., Leutert, T.J., Marquardt, J., Ziegler, M., Agterhuis, T., Lourens, L.J., Rae, J.W.B., Barnet, J., Tripati, A., Bernasconi, S.M., 2022. Cenozoic evolution of deep ocean temperature from clumped isotope thermometry. Science (1979) 377, 86–90. https://doi.org/10.1126/SCIENCE.ABK0604/SUPPL_FILE/SCIENCE.ABK0604_DATA_S1_TO_S3.ZIP

Meinicke, N., Ho, S.L., Hannisdal, B., Nürnberg, D., Tripati, A., Schiebel, R., Meckler, A.N., 2020. A robust calibration of the clumped isotopes to temperature relationship for foraminifers. Geochim Cosmochim Acta 270, 160–183. https://doi.org/10.1016/J.GCA.2019.11.022

Meinicke, N., Reimi, M.A., Ravelo, A.C., Meckler, A.N., 2021. Coupled Mg/Ca and Clumped Isotope Measurements Indicate Lack of Substantial Mixed Layer Cooling in the Western Pacific Warm Pool During the Last ~5 Million Years. Paleoceanogr Paleoclimatol 36, e2020PA004115. https://doi.org/10.1029/2020PA004115

Mejía, L.M., Ziveri, P., Cagnetti, M., Bolton, C., Zahn, R., Marino, G., Martínez-Méndez, G., Stoll, H., 2014. Effects of midlatitude westerlies on the paleoproductivity at the Agulhas Bank slope during the penultimate glacial cycle: Evidence from coccolith Sr/Ca ratios. Paleoceanography 29. https://doi.org/10.1002/2013PA002589

Mignot, A., Ferrari, R., Claustre, H., 2018. Floats with bio-optical sensors reveal what processes trigger the North Atlantic bloom. Nat Commun 9, 1–9. https://doi.org/10.1038/s41467-017-02143-6

Müller, I.A., Rodriguez-Blanco, J.D., Storck, J.C., do Nascimento, G.S., Bontognali, T.R.R., Vasconcelos, C., Benning, L.G., Bernasconi, S.M., 2019. Calibration of the oxygen and clumped isotope thermometers for (proto-)dolomite based on synthetic and natural carbonates. Chem Geol 525, 1–17. https://doi.org/10.1016/J.CHEMGEO.2019.07.014

Müller, P.J., Kirst, G., Ruhland, G., von Storch, I., Rosell-Melé, A., 1998. Calibration of the alkenone paleotemperature index UK'37 based on core-tops from the eastern South Atlantic and the global ocean (60°N-60°S). Geochim Cosmochim Acta 62, 1757–1772. https://doi.org/10.1016/S0016-7037(98)00097-0

Peral, M., Bassinot, F., Daëron, M., Blamart, D., Bonnin, J., Jorissen, F., Kissel, C., Michel, E., Waelbroeck, C., Rebaubier, H., Gray W. R, 2022. On the combination of the planktonic foraminiferal Mg/Ca, clumped (Δ47) and conventional (δ18O) stable isotope paleothermometers in palaeoceanographic studies. Geochim Cosmochim Acta Preprint. https://doi.org/https://doi.org/10.31223/X5VK82

Peral, M., Daëron, M., Blamart, D., Bassinot, F., Dewilde, F., Smialkowski, N., Isguder, G., Bonnin, J., Jorissen, F., Kissel, C., Michel, E., Vázquez Riveiros, N., Waelbroeck, C., 2018. Updated calibration of the clumped isotope thermometer in planktonic and benthic foraminifera. Geochim Cosmochim Acta 239, 1–16. https://doi.org/10.1016/j.gca.2018.07.016

Piasecki, A., Bernasconi, S.M., Grauel, A., Hannisdal, B., Ho, S.L., Leutert, T.J., Marchitto, T.M., Meinicke, N., Tisserand, A., Meckler, N., 2019. Application of clumped isotope thermometry to benthic foraminifera. Geochemistry, Geophysics, Geosystems 20, 2082–2090. https://doi.org/10.1029/2018GC007961

Poulton, A.J., Holligan, P.M., Charalampopoulou, A., Adey, T.R., 2017. Coccolithophore ecology in the tropical and subtropical Atlantic Ocean: New perspectives from the Atlantic meridional transect (AMT) programme. Prog Oceanogr 158, 150–170. https://doi.org/10.1016/J.POCEAN.2017.01.003

Prahl, F.G., Muehlhausen, L.A., Zahnle, D.L., 1988. Further evaluation of long-chain alkenones as indicators of paleoceanographic conditions. Geochim Cosmochim Acta 52, 2303–2310. https://doi.org/10.1016/0016-7037(88)90132-9

Rebotim, A., Voelker, A.H.L., Jonkers, L., Waniek, J.J., Meggers, H., Schiebel, R., Fraile, I., Schulz, M., Kucera, M., 2017. Factors controlling the depth habitat of planktonic foraminifera in the subtropical eastern North Atlantic. Biogeosciences 14, 827–859. https://doi.org/10.5194/bg-14-827-2017

Richter, F.M., Liang, Y., 1993. The rate and consequences of Sr diagenesis in deep-sea carbonates. Earth Planet Sci Lett 117, 553–565. https://doi.org/10.1016/0012-821X(93)90102-F

Rodríguez-Sanz, L., Bernasconi, S.M., Marino, G., Heslop, D., Müller, I.A., Fernandez, A., Grant, K.M., Rohling, E.J., 2017. Penultimate deglacial warming across the Mediterranean Sea revealed by clumped isotopes in foraminifera. Scientific Reports 2017 7:1 7, 1–11. https://doi.org/10.1038/s41598-017-16528-6

Romero, O., Boeckel, B., Donner, B., Lavik, G., Fischer, G., Wefer, G., 2002. Seasonal productivity dynamics in the pelagic central Benguela System inferred from the flux of carbonate and silicate organisms. Journal of Marine Systems 37, 259–278. https://doi.org/10.1016/S0924-7963(02)00189-6

Rommerskirchen, F., Condon, T., Mollenhauer, G., Dupont, L., Schefuss, E., 2011. Miocene to Pliocene development of surface and subsurface temperatures in the Benguela Current system. Paleoceanography 26. https://doi.org/10.1029/2010PA002074

Schauble, E.A., Ghosh, P., Eiler, J.M., 2006. Preferential formation of 13C-18O bonds in carbonate minerals, estimated using first-principles lattice dynamics. Geochim Cosmochim Acta 70, 2510–2529. https://doi.org/10.1016/j.gca.2006.02.011

Schlitzer, R., 2021. Ocean Data View, odv.awi.de.

Schouten, S., Hopmans, E.C., Sinninghe Damsté, J.S., 2013. The organic geochemistry of glycerol dialkyl glycerol tetraether lipids: A review. Org Geochem 54, 19–61. https://doi.org/10.1016/j.orggeochem.2012.09.006

Spero, H.J., Mielke, K.M., Kalve, E.M., Lea, D.W., Pak, D.K., 2003. Multispecies approach to reconstructing eastern equatorial Pacific thermocline hydrography during the past 360 kyr. Paleoceanography 18, 1022. https://doi.org/10.1029/2002PA000814

Spooner, P.T., Guo, W., Robinson, L.F., Thiagarajan, N., Hendry, K.R., Rosenheim, B.E., Leng, M.J., 2016. Clumped isotope composition of cold-water corals: A role for vital effects? Geochim Cosmochim Acta 179, 123–141. https://doi.org/10.1016/J.GCA.2016.01.023

Tagliavento, M., John, C.M., Stemmerik, L., 2019. Tropical temperature in the Maastrichtian Danish Basin: Data from coccolith Δ47 and δ18O. Geology 47, 1074–1078. https://doi.org/10.1130/G46671.1

Tierney, J.E., Sinninghe Damsté, J.S., Pancost, R.D., Sluijs, A., Zachos, J.C., 2017a. Eocene temperature gradients. Nat Geosci 10, 538–539. https://doi.org/10.1038/ngeo2997

Tierney, J.E., Tingley, M.P., 2018. BAYSPLINE: A New Calibration for the Alkenone Paleothermometer. Paleoceanogr Paleoclimatol 33, 281–301. https://doi.org/10.1002/2017PA003201

Tripati, A.K., Eagle, R.A., Thiagarajan, N., Gagnon, A.C., Bauch, H., Halloran, P.R., Eiler, J.M., 2010. 13C-18O isotope signatures and "clumped isotope" thermometry in foraminifera and coccoliths. Geochim Cosmochim Acta 74, 5697–5717. https://doi.org/10.1016/j.gca.2010.07.006

WOA, 2018. World Ocean Atlas 2018 Data Access [WWW Document]. URL https://www.ncei.noaa.gov/access/world-ocean-atlas-2018/ (accessed 4.4.22).

York, D., Evensen, N., López-Martínez, M., de Basabe Delgado, J., 2004. Unified equations for the slope, intercept, and standard errors of the best straight line. Am J Phys 72. https://doi.org/10.1119/1.1632486

1004 Zhang, H., Liu, C., Mejía, L.M., Stoll, H., 2021. Technical note: Accelerate coccolith
1005 size separation via repeated centrifugation. Biogeosciences 18, 1909–1916.
1006 https://doi.org/10.5194/BG-18-1909-2021
1007 Zhu, J., Poulsen, C.J., Tierney, J.E., 2019. Simulation of Eocene extreme warmth and
1008 high climate sensitivity through cloud feedbacks. Sci Adv 5.
1009 https://doi.org/10.1126/SCIADV.AAX1874/SUPPL_FILE/AAX1874_TABLES_S
1010 1_AND_S2.XLSX
1011 Ziveri, P., Stoll, H., Probert, I., Klaas, C., Geisen, M., Ganssen, G., Young, J., 2003.
1012 Stable isotope 'vital effects' in coccolith calcite. Earth Planet Sci Lett 210, 137–
1013 149. https://doi.org/10.1016/S0012-821X(03)00101-8
1014